The Plant Cell, Vol. 24: 4083–4095, October 2012, www.plantcell.org

RETINOBLASTOMA RELATED1 Regulates Asymmetric Cell Divisions in *Arabidopsis*[C][W][OA]

Annika K. Weimer,[a,1] Moritz K. Nowack,[b,c,1] Daniel Bouyer,[a] Xin'Ai Zhao,[a] Hirofumi Harashima,[a,d] Sadaf Naseer,[e] Freya De Winter,[b,c] Nico Dissmeyer,[a,2] Niko Geldner,[e] and Arp Schnittger[a,d,3]

[a] Department of Molecular Mechanisms of Phenotypic Plasticity, Institut de Biologie Moléculaire des Plantes du Centre National de la Recherche Scientifique, IBMP, Unité propre de recherche 2357, Université de Strasbourg, F-67084 Strasbourg cedex, France
[b] Department of Plant Systems Biology, Vlaams Instituut voor Biotechnologie, B-9052 Ghent, Belgium
[c] Department of Plant Biotechnology and Bioinformatics, Ghent University, B-9052 Ghent, Belgium
[d] Trinationales Institut für Pflanzenforschung, Institut de Biologie Moléculaire des Plantes du Centre National de la Recherche Scientifique, IBMP, F-67084 Strasbourg cedex, France
[e] Department of Plant Molecular Biology, University of Lausanne, CH-1015 Lausanne, Switzerland

Formative, also called asymmetric, cell divisions produce daughter cells with different identities. Like other divisions, formative divisions rely first of all on the cell cycle machinery with centrally acting cyclin-dependent kinases (CDKs) and their cyclin partners to control progression through the cell cycle. However, it is still largely obscure how developmental cues are translated at the cellular level to promote asymmetric divisions. Here, we show that formative divisions in the shoot and root of the flowering plant *Arabidopsis thaliana* are controlled by a common mechanism that relies on the activity level of the Cdk1 homolog CDKA;1, with medium levels being sufficient for symmetric divisions but high levels being required for formative divisions. We reveal that the function of CDKA;1 in asymmetric cell divisions operates through a transcriptional regulation system that is mediated by the *Arabidopsis* Retinoblastoma homolog RBR1. RBR1 regulates not only cell cycle genes, but also, independent of the cell cycle transcription factor E2F, genes required for formative divisions and cell fate acquisition, thus directly linking cell proliferation with differentiation. This mechanism allows the implementation of spatial information, in the form of high kinase activity, with intracellular gating of developmental decisions.

INTRODUCTION

The development of multicellular organisms requires a tight coordination of cell proliferation with growth and differentiation (Harashima and Schnittger, 2010). A paradigm for the need of this coordination are formative, also called asymmetric or unequal, cell divisions in which one cell will give rise to two cells each with different cell fates (Abrash and Bergmann, 2009; Knoblich, 2010; De Smet and Beeckman, 2011). Formative divisions are typically found in stem cell niches and the cell lineages originating from stem cells. A typical example is found in the *Arabidopsis thaliana* root meristem, where stem cells are grouped around a quiescent center (Benfey and Scheres, 2000). While most root tissues are organized into files of cells that are derived each from one of these stem cells, the cell files of both the endodermis and the cortex layers originate from one common cortex-endodermis initial. Thus, instead of an anticlinal division that is perpendicular to the surface of the root and contributes to the length of a cell file, the division plane in the cortex-endodermis initial daughter cell is shifted by 90°, resulting in a periclinal cell division (i.e., a division that generates two cells parallel to the surface of the root with different fates, namely, cortex and endodermis).

Formative divisions can also be found during the development of aerial plant structures, and a representative case are the cell divisions in the stomata lineage. This cell lineage produces stomata, gas exchange pores formed by two guard cells, as well as epidermal pavement cells (Bergmann and Sack, 2007). Stomata are produced via a series of asymmetric divisions, the first of which occurs in a parent meristemoid mother cell to produce a meristemoid cell. The meristemoid cell is a transit-amplifying cell that may divide asymmetrically several times, each time producing a new epidermal cell and regenerating the meristemoid. The meristemoid ultimately differentiates into a guard mother cell that divides symmetrically to produce two guard cells.

Formative divisions, like any other type of division, rely on the cell cycle machinery with centrally acting cyclin-dependent kinases (CDKs) and their cyclin cofactors to promote S phase and mitosis. In *Arabidopsis*, five CDKs have been identified to be the core cell cycle regulators. CDKA;1 controls entry into M phase and especially entry into S phase by phosphorylating RETINOBLASTOMA RELATED1 (RBR1), the *Arabidopsis* homolog of the human tumor suppressor Retinoblastoma (Nowack et al.,

[1] These authors contributed equally to this work.
[2] Current address: Leibniz Institute of Plant Biochemistry, Weinberg 3, D-06120 Halle (Saale), Germany.
[3] Address correspondence to arp.schnittger@ibmp-cnrs.unistra.fr.
The author responsible for distribution of materials integral to the findings presented in this article in accordance with the policy described in the Instructions for Authors (www.plantcell.org) is: Arp Schnittger (arp.schnittger@ibmp-cnrs.unistra.fr).
[C] Some figures in this article are displayed in color online but in black and white in the print edition.
[W] Online version contains Web-only data.
[OA] Open Access articles can be viewed online without a subscription.
www.plantcell.org/cgi/doi/10.1105/tpc.112.104620

2012). In the nonphosphorylated state, RBR1 represses the action of the transcription factor E2F that activates the expression of many genes required for DNA replication, such as F-BOX PROTEIN17 (FBL17), PROLIFERATING CELL NUCLEAR ANTIGEN (PCNA), and MINICHROMOSOME MAINTENANCE PROTEIN5 (MCM5) (Gutzat et al., 2012; Zhao et al., 2012). CDKA;1 action for S phase entry is backed up by the two redundantly acting CDKB1s (CDKB1;1 and CDKB1;2) (Nowack et al., 2012). CDKB1s also function in the control of M phase and the analysis of loss-of-function as well as dominant-negative alleles have in particular revealed a role in the last (i.e., symmetric) division during stomata development (Boudolf et al., 2004; Xie et al., 2010). CDKB2s (CDKB2;1 and CDKB2;2) appear to be M phase specific, as judged by their strong cell cycle phase-dependent expression pattern (Boudolf et al., 2004; Menges et al., 2005; Xie et al., 2010). CDKB2 action was found to be specifically required for the function of the shoot apical meristem (Andersen et al., 2008). CDKs by themselves have almost no kinase activity and require the binding of a cyclin partner. In *Arabidopsis*, there are 30 cyclins and almost all of them can bind to each of the five core CDKs (Van Leene et al., 2011). However, the number of functional pairs might be smaller, as suggested by in vitro kinase assays (Harashima and Schnittger, 2012).

Recent evidence indicated a special role for some core cell cycle regulators in asymmetric cell divisions. *CYCLIN D6;1* (*CYCD6;1*) was found to be specifically expressed in the cortex-endodermis initial daughter cells, and in *cycd6;1* mutants, this division is delayed (Sozzani et al., 2010). Conversely, CYCD4;1 appears to modulate divisions that initiate a stomata lineage and overexpression stimulated the production of stomata (Kono et al., 2007). However, how cell cycle regulators can translate developmental cues at the cellular level to promote formative divisions has remained largely obscure.

Here, we present a general mechanism of how extracellular information can be integrated with an intracellular gene regulatory network to execute formative divisions. We show that RBR1 regulates both cell cycle and cell differentiation genes. RBR1 activity is predominantly regulated by CDKA;1, giving rise to a CDKA;1 dose-dependent model of symmetric versus asymmetric cell divisions that hence allows the developmentally programmed activation of the cell cycle machinery to promote formative cell divisions.

RESULTS

Reduction of CDKA;1 Activity Affects Formative Cell Divisions in the Root

Weak loss-of-function (hypomorphic) alleles and allelic series, especially of essential regulators, are powerful tools to dissect developmental processes and to infer gene function in vivo. Previously, we addressed the posttranslational regulation of the central cell cycle kinase CDKA;1 in *Arabidopsis* by exchanging amino acids that are known from work in yeast and metazoans to be subject to inhibitory and stimulatory phosphorylation events in CDKA;1 homologs (Pines, 1995; Morgan, 1997). Of key importance for the activation of this type of kinase is the phosphorylation in the activation loop, also called the T-loop, at residue Thr-161 of CDKA;1 in *Arabidopsis*, or at the corresponding position (e.g., Thr-169 of CDC28 in *Saccharomyces cerevisiae* or Thr-167 of Cdc2 in *Schizosaccharomyces pombe*). Conversely, phosphorylation of the residues Thr-14 and Tyr-15 and the corresponding positions in the regulatory loop, also called the P-loop, has a strong inhibitory function. The expression of a *CDKA;1* variant in which Thr-161 was replaced with the nonphosphorylatable amino acid Val (*cdka;1*$^{-/-}$ *Pro*$_{CDKA;1}$:*CDKA;1*^{T161V}) could not rescue *cdka;1* mutants, consistent with a requirement of Thr-161 phosphorylation for kinase activation (Dissmeyer et al., 2007). A variant that mimicked a phosphorylated amino acid (i.e., one in which Thr-161 was replaced with the negatively charged amino acid Asp; *cdka;1*$^{-/-}$ *Pro*$_{CDKA;1}$:*CDKA;1*^{T161D}) could rescue the *cdka;1* mutant, albeit only partially, giving rise to a hypomorphic *cdka;1* mutant designated *D* in the following (Dissmeyer et al., 2007). Conversely, the exchanges of Thr-14 and Tyr-15 with Asp and Glu mimicked an inhibited CDKA;1 and, after transformation of the respective cDNA expression construct into *cdka;1* mutants, resulted in a second hypomorphic mutant (*cdka;1*$^{-/-}$ *PRO*$_{CDKA;1}$:*CDKA;1*$^{T14D;Y15E}$), designated *DE* in the following (Dissmeyer et al., 2009).

While null mutants of *CDKA;1* are severely compromised and not viable on soil (Nowack et al., 2006, 2012), hypomorphic *CDKA;1* mutants *D* and *DE* are much less affected and in general form all of the organs and cell types of wild-type plants (Figure 1A). However, when analyzing in detail the root architecture of these hypomorphic mutants, we found specific developmental defects. Whereas the formative division of a cortex-endodermis initial daughter is rapidly executed in the wild type, the division was delayed in weak loss-of-function *cdka;1* mutants, resulting in a unique phenotype with files of up to three additional cells between the initial and the beginning of two separated endodermis and cortex layers (Figures 2A to 2C, Table 1; see Supplemental Table 1 online). Initial daughter cells are marked by the expression of *CYCD6;1* (Sozzani et al., 2010), and we observed that a *CYCD6;1* reporter was active in the newly arising cell files between the quiescent center and the eventually forming endodermis and cortex cell files of weak *cdka;1* loss-of-function alleles, implying that they have initial daughter fate (Figures 2D and 2E).

The generation of additional initial daughter cells and the delayed formation of separate endodermis and cortex files, however, did not interfere with subsequent differentiation steps, as seen by the proper formation of the Casparian strip, the hallmark of the endodermis layer (see Supplemental Figures 1A to 1F online). In addition, we found that the endodermis marker SCARECROW (SCR) and the cortex marker CORTEX2 (CO2) become expressed in the respective cell files in both hypomorphic *cdka;1* mutants (Figures 2F and 2G; see Supplemental Figures 2A and 2B online). Thus, the appearance of daughter cell files in hypomorphic *cdka;1* represents a specific defect in formative cell division of the cortex-endodermis initial daughter cell.

The Phenotype of Weak *cdka;1* Loss-of-Function Alleles Becomes Stronger over Time

The *Arabidopsis* root meristem is established during embryo development, and wild-type embryos at maturity contain

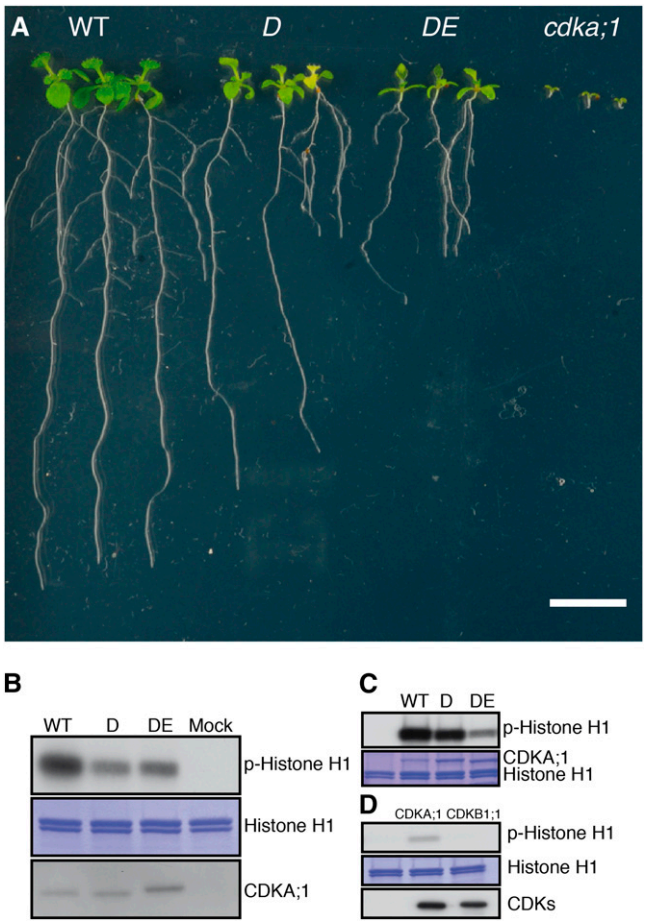

Figure 1. Allelic Series of *cdka;1* Mutants.

(A) Ten-day-old wild-type (WT), *D*, *DE*, and homozygous *cdka;1* mutant plants (from left to right). Bar = 1 cm.

(B) p13^{suc1}-associated protein kinase activity is strongest in wild-type extracts, while extracts from D plants have higher activity than those from DE extracts as revealed by autoradiography (top panel). Coomassie blue staining (middle panel) shows equal loading of the substrate histone H1. Equal purification levels of CDKs were quantified by protein blot with the anti-PSTAIR antibody (bottom panel). Protein extraction buffer was incubated with p13^{suc1} beads as a mock.

(C) In vitro kinase assays show that the hypomorphic *cdka;1* mutant *D* has less activity than the wild type but more than the hypomorphic *cdka;1* mutant *DE* (autoradiography top). Coomassie blue staining (bottom) shows equal loading of the substrate histone H1 and the different CDKA;1 versions.

(D) In vitro kinase assays of CDK-CYCD6;1 complexes reveal that CYCD6;1 has activity with CDKA;1 but not with CDKB1;1 against histone H1 (autoradiography top). Coomassie blue staining (middle) shows equal loading of the substrate histone H1. Quantification with Strep-Tactin HRP (bottom) reveals equal amounts of CDKA;1 and CDKB1;1 bound to CYCD6;1.

a cortex-endodermis initial and a cortex-endodermis initial daughter cell. After germination, root meristems of *Arabidopsis* expand in the following 5 to 6 d and then plateau (Ubeda-Tomás et al., 2009). When analyzing the embryonic root meristem in both hypomorphic *cdka;1* mutants, we found that the pattern of the formative division of the cortex-endodermis initial daughter was indistinguishable from that of the wild type, suggesting that the mutant phenotype would become more severe over time (Figures 3A to 3C). Indeed, roots analyzed at 10 d after germination showed significantly ($P < 0.001$) longer files of undivided initial daughter cells than roots examined at 5 d after germination (Figure 3D). Remarkably, we never observed that any cell but the top-most cell within the single file of initial daughter cells divided asymmetrically, suggesting that the specific position neighboring the already established separated cortex and endodermis files provides spatial cues for the asymmetric division (Figure 2C). This top-most cell never divided anticlinally (i.e., symmetrically), as judged by the continuously increasing cell sizes in the files of mutant initial daughter cells. Thus, we conclude that in *cdka;1* mutants, the different cell division programs within the root meristem are uncoupled: The initials continue to divide and produce daughter cells, but the formative division of the initial daughter cell occurs in *cdka;1* mutants with a lower rate, resulting in growing files of daughter cells and a separation of cell production and differentiation.

Formative Divisions in the Root Meristem Depend on CDKA;1 Dosage

The stronger phenotype of the *DE* versus *D* hypomorphic *cdka;1* mutant plants suggested that the asymmetric division of a cortex-endodermis initial daughter correlates with the activity levels of CDKA;1. In vitro kinase reactions with both mutant kinase versions and CDK activities extracted from both hypomorphic mutants revealed that *D* has higher activity than *DE*, although still markedly less activity than wild-type CDKA;1 (Figures 1B and 1C). This series of kinase activity also correlated with overall plant growth (i.e., wild-type plants are bigger than *D*, and *D* plants grows larger than *DE*) (Figure 1A). To further test a possible CDKA;1 kinase dose dependency of the formative division of an initial daughter cell, we analyzed roots of homozygous *cdka;1* null mutants that can be grown on agar plates but are even smaller than *DE* plants (Figure 1A) (Nowack et al., 2012). In homozygous mutants, the root meristem architecture is severely compromised, hampering quantitative morphological analyses, but in several optical sections, the formative division of the initial daughter was more strongly delayed than in the weak loss-of-function mutants or even failed completely (Figure 2H; see Supplemental Figures 2C and 2F online). Thus, the formative divisions of the initial daughter cells depend on the dose of CDKA;1 activity.

Since the embryonic root meristem was correctly established in hypomorphic *cdka;1* mutants, and even in *cdka;1* null mutants the initial daughter cells occasionally divided asymmetrically, we asked whether other CDKs than CDKA;1 are also involved in this cell division. Based on the finding that *CDKB1* can partially compensate for the loss of *CDKA;1* (Nowack et al., 2012), we first analyzed homozygous *cdka;1* mutants in which *CDKB1* was expressed from the *CDKA;1* promoter. Along with a general restoration of the root meristem, the formative division of the initial daughter cells was partially restored (Figure 2J, Table 1). Accordingly, we found that *cdkb1;1 cdkb1;2* double mutants showed a mild delay in the division of the initial daughter (Table 1; see Supplemental Table 1 online). However, we never observed

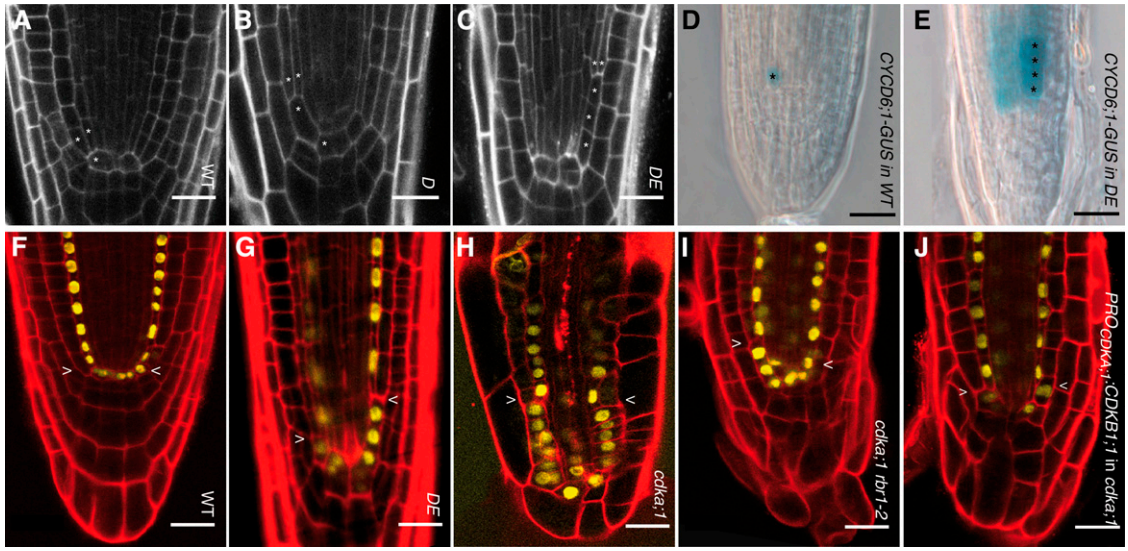

Figure 2. Formative Divisions in the Root Correlate with CDKA;1 Activity Levels.

(A) In wild-type (WT) roots, the cortex-endodermis initial next to the quiescent center produces a cortex-endodermis initial daughter cell that rapidly divides asymmetrically, giving rise to a cortical and endodermal cell.
(B) and **(C)** In weak loss-of-function *cdka;1* mutants, the initial daughter division is delayed so that an initial daughter is present for a longer time **(B)**, or due to continued divisions of the initial **(C)**, files of undivided initial daughter cells are generated.
(D) CYCD6;1:GUS marks the initial daughter in the wild type.
(E) The additional cell files in DE are also marked by CYCD6;1:GUS, indicating their fate as initial daughters.
(F) to **(J)** The expression pattern of Pro_{SCR}:*SCR*:*YFP*, marking quiescent center, cortex-endodermis initial, cortex-endodermis initial daughter, and endodermal cells, is similar in the wild type **(F)**, weak loss-of-function *cdka;1* mutants **(G)**, null *cdka;1* mutants **(H)**, and *cdka;1 rbr1-2* **(I)** and $Pro^{CDKA;1}$:CDKB1;1 **(J)**.
In **(A)** to **(C)**, a single asterisk indicates cortex-endodermis initials and their daughter cells. The formative division gives rise to an endodermis and cortex cell, which is marked by two asterisks. Bars = 20 μm.

files of undivided initial daughter cells in the *cdkb1* double mutant, and even the loss of both *CDKB1* genes in hypomorphic *cdka;1* mutants (*cdka;1*$^{-/-}$ $Pro_{CDKA;1}$*CDKA;1*$^{T14D;Y15E+/+}$ *cdkb1;1*$^{-/-}$ *cdkb1;2*$^{-/-}$) did not enhance the mutant phenotype of the weak *cdka;1* loss-of-function alleles (Table 1). Thus, we conclude that it is CDKA;1 and not CDKB1;1/CDKB1;2 that plays a central role during formative divisions. However, CDKB1s contribute to the fast execution of the initial daughter division, additionally

Table 1. Division of Cortex-Endodermis Initial Daughter Cells until Differentiation of Cortex and Endodermis

	No. of Divisions of a Cortex-Endodermis Initial Daughter Cell until Differentiation (in %)				
Genotype	1	2	3	4	*n*
The wild type	100	0	0	0	50
cdka;1	n.a.[a]	n.a.	n.a.	n.a.	0[b]
DE	25	42	25	8	72
D	53	42	5	0	72
cdkb1;1 cdkb1;2	98	2	0	0	40
DE cdkb1;1 cdkb1;2	17	50	28	5	36
$Pro_{CDKA;1}$:*CDKB1;1* in *cdka;1*	60	25	5	10	40
rbr1-2	100	0	0	0	92
DE rbr1-2	79	14	7	0	28
rbr1-2 cdka;1	86	0	7	7	28
cycd6;1	94	6	0	0	36
D cycd6;1	65	23	9	3	40
cdkb1;1 cdkb1;2 cycd6;1	98	2	0	0	43

[a]n.a.,not analyzable
[b]Twenty-five roots/50 cortex-endodermis initial daughter divisions analyzed.

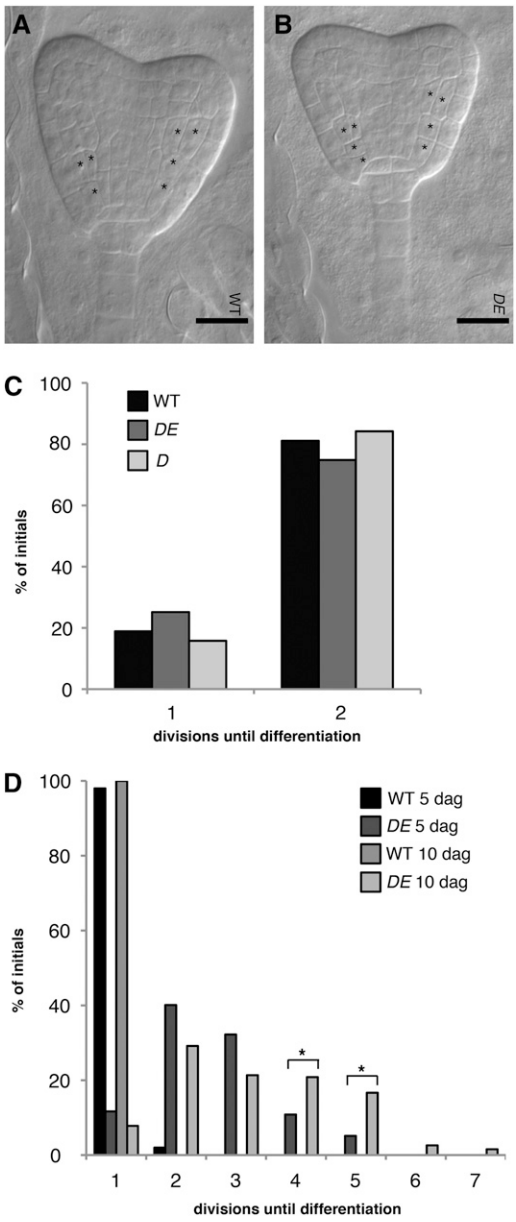

Figure 3. Time Course of Initial Daughter Division in Weak *cdka;1* Alleles.

(A) Mature wild-type (WT) embryos contain an initial and an initial daughter.

(B) The weak loss-of-function *cdka;1* mutant *DE* is indistinguishable from the wild type with respect to the embryonic initial and initial daughter pattern.

(C) Quantification revealed no significant difference of initial daughter division between wild-type and DE plants.

(D) The mutant phenotype of *DE* becomes stronger over time. At day 5, DE is significantly different from the wild type ($P < 0.001$). Files between QC and the endodermis-cortex specification contain up to five cells at 5 d after germination (dag) but up to seven cells after the 10th day. Asterisks indicate significant differences within a 5% confidence interval.

In **(A)** and **(B)**, a single asterisk indicates cortex-endodermis initials and their daughter cells. The formative division gives rise to an endodermis and cortex cell, which is marked by two asterisks.

stressing the importance of a CDK activity-dependent mechanism for this division.

Since CYCD6;1 is specifically involved in the formative division of the initial daughter cells in *Arabidopsis* (Sozzani et al., 2010), we next asked whether CDKA;1 or CDKB1s operates together with CYCD6;1. Although both kinases coprecipitated in vitro with CYCD6;1, only the combination with CDKA;1 showed kinase activity, underscoring the central function of CDKA;1 in the division of the initial daughter (Figure 1D). However, removal of CYCD6;1 activity in hypomorphic *cdka;1* mutant plants did not significantly enhance the *cdka;1* mutant phenotype, indicating that additional cyclins are involved in this asymmetric division, likely each with a small contribution to the overall CDKA;1 activity (Table 1; see Supplemental Table 1 online). The assisting role of CDKB1s and CYCD6;1 to the asymmetric division of the initial daughter was further supported by the observation that the *cdkb1;1 cdkb1;2 cycd6;1* triple mutant did not show undivided initial daughter cells (Table 1; see Supplemental Table 1 online).

Formative Divisions Are Regulated by RBR1

The requirement of high CDK activity levels argued that one or more CDK substrates are responsible for the formative division of the cortex-endodermis initial daughter. Recently, some CDKA;1 substrates were identified in *Arabidopsis*, and especially RBR1 was found to be a crucial target of CDKA;1 (Nowack et al., 2012; Pusch et al., 2012). If the inactivation of RBR1 by CDKA;1-mediated phosphorylation is of central importance for the execution of the formative division of the initial daughter cell, a reduction of RBR1 levels should at least partially restore the mutant phenotype of weak *cdka;1* loss-of-function mutants. Therefore, we introgressed a *rbr1* mutant into hypomorphic *cdka;1* mutants; indeed, we found that *DE rbr1* double mutants showed a strong restoration of the wild-type division pattern of the initial daughter cell (Table 1; see Supplemental Table 1 online). Strikingly, formative division of the initial daughter was, even in homozygous *cdka;1*$^{-/-}$ null mutants, largely restored when *RBR1* was depleted (Figure 2I, Table 1; see Supplemental Figure 2D and Supplemental Table 1 online). As RBR1 exerts many of its functions as a transcriptional regulator, our results suggest a transcriptional base of the observed delay in the formative division of an initial daughter cell.

Intensive work over the last few years has revealed that the transcription factors *SHORTROOT* (*SHR*) and *SCR* regulate the asymmetric division and subsequent fate specification of the initial daughter cells (Ten Hove and Heidstra, 2008; De Smet and Beeckman, 2011). Thus, the direct regulation of the asymmetric cell division by RBR1 could conceivably operate by modulating the *SHR* and *SCR* pathway. We therefore tested whether RBR1 would bind to the promoter regions of a cluster of six genes that were recently identified as SHR targets: *At4g01330*, *CYCD6;1*, *MAGPIE* (*MGP*), *NUTCRACKER* (*NUC*), *SCARECROW LIKE3* (*SCL3*), and *SCR* itself (see Supplemental Figure 3 online) (Sozzani et al., 2010). To this end, we performed chromatin immunoprecipitation (ChIP) experiments using an antibody directed against red fluorescent protein (RFP) in transgenic plants that produce an RBR1:RFP fusion protein (Ingouff et al., 2006). As expected, we observed in ChIP-PCR experiments RBR1 binding to the known RBR1 targets

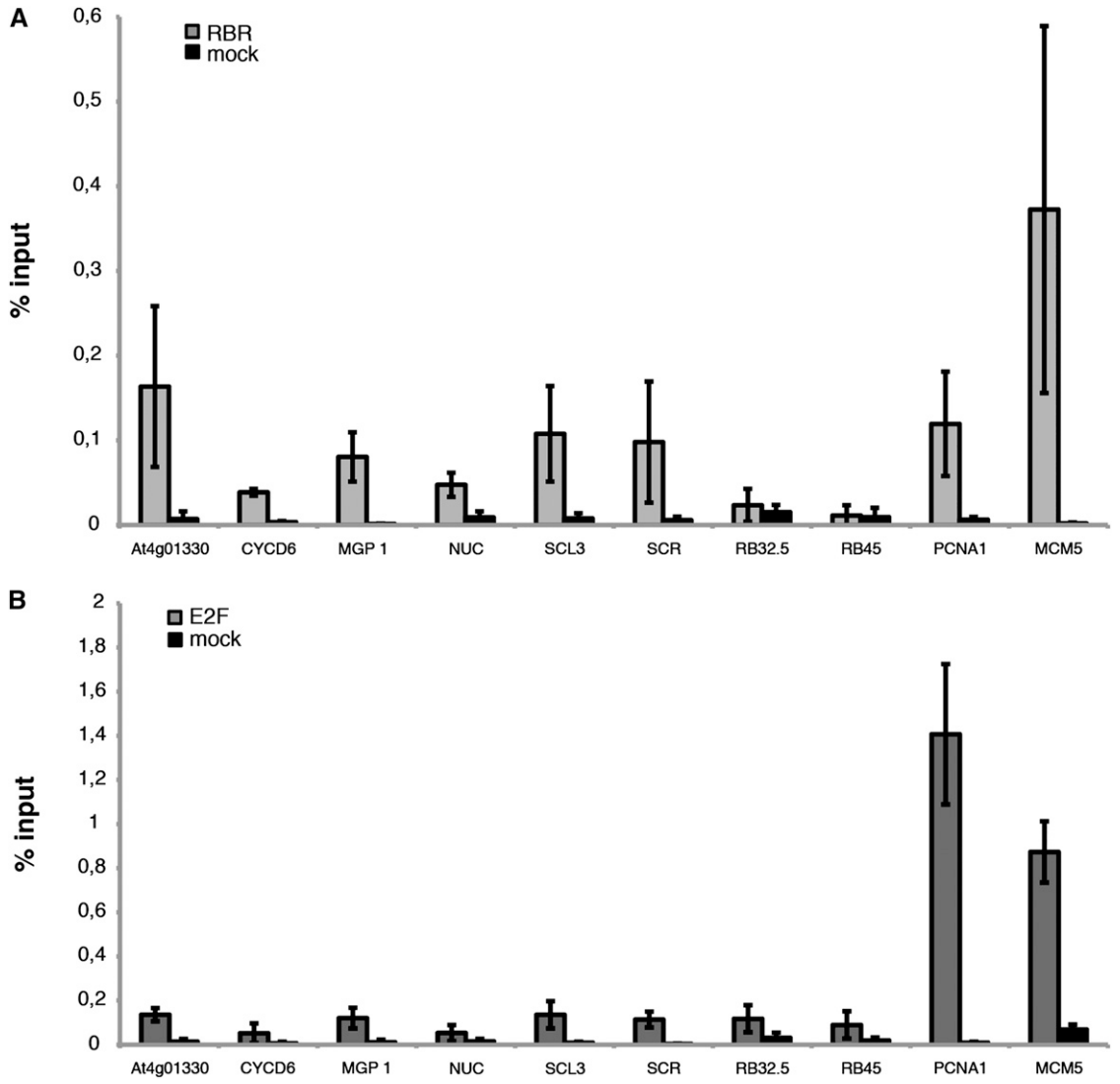

Figure 4. RBR1 Binds to Cell Cycle Genes and Genes Involved in Cell Differentiation in the Root.

(A) ChIP of Pro_{RBR1}:*RBR1*:*RFP* seedlings using an anti-RFP antibody. The promoter regions of *At4G01330*, *MGP1*, *SCL3*, *SCR*, and the cell cycle genes *PCNA1* and *MCM5* are bound by RBR1, whereas the heterochromatic regions (RB32.5 and RB45) show no difference between mock and treatment. **(B)** RBR1 targets MCM5 and PCNA1 can also be detected with an E2FA antibody. However, no enrichment could be observed for the SHR targets tested in **(A)**.

FBL17, *MCM5*, and *PCNA1* (Nowack et al., 2012; Zhao et al., 2012). Fragments further upstream or downstream of the known RBR1 binding site could not be amplified. Remarkably, the promoter region that was previously identified as being bound by SHR could be specifically amplified for *At4g01330* and *SCL3*. However, we could not find evidence for binding of RBR1 to the promoter region of the presumptive SHR/SCR target gene *CYCD6;1* (see Supplemental Figure 3 online).

Next, we quantified the binding of RBR1 to the promoter fragments containing a SHR binding site by ChIP–quantitative PCR (Figure 4A; see Supplemental Figure 3 online). Two heterochromatic loci were used as negative controls and showed no enrichment in our ChIP assays. A weak enrichment was obtained for *CYCD6;1* and *NUC*. Although we cannot exclude a weak binding of RBR1 to these genes, we conclude that the here-seen weak enrichment is due to unspecific binding of the antibody based on the failure to amplify the same fragments in the more stringent ChIP-PCR. Notably, *At4g01330*, *MGP*, *SCL3*, and *SCR* were at least 5 times more enriched than the negative control and showed enrichment similar to the known RBR1 target PCNA1, corroborating them as RBR1 targets.

RBR1 generally counteracts E2F function in cell cycle regulation (Weinberg, 1995), and the RBR1 targets *MCM5* as well as *PCNA1* could also be precipitated with an antibody recognizing

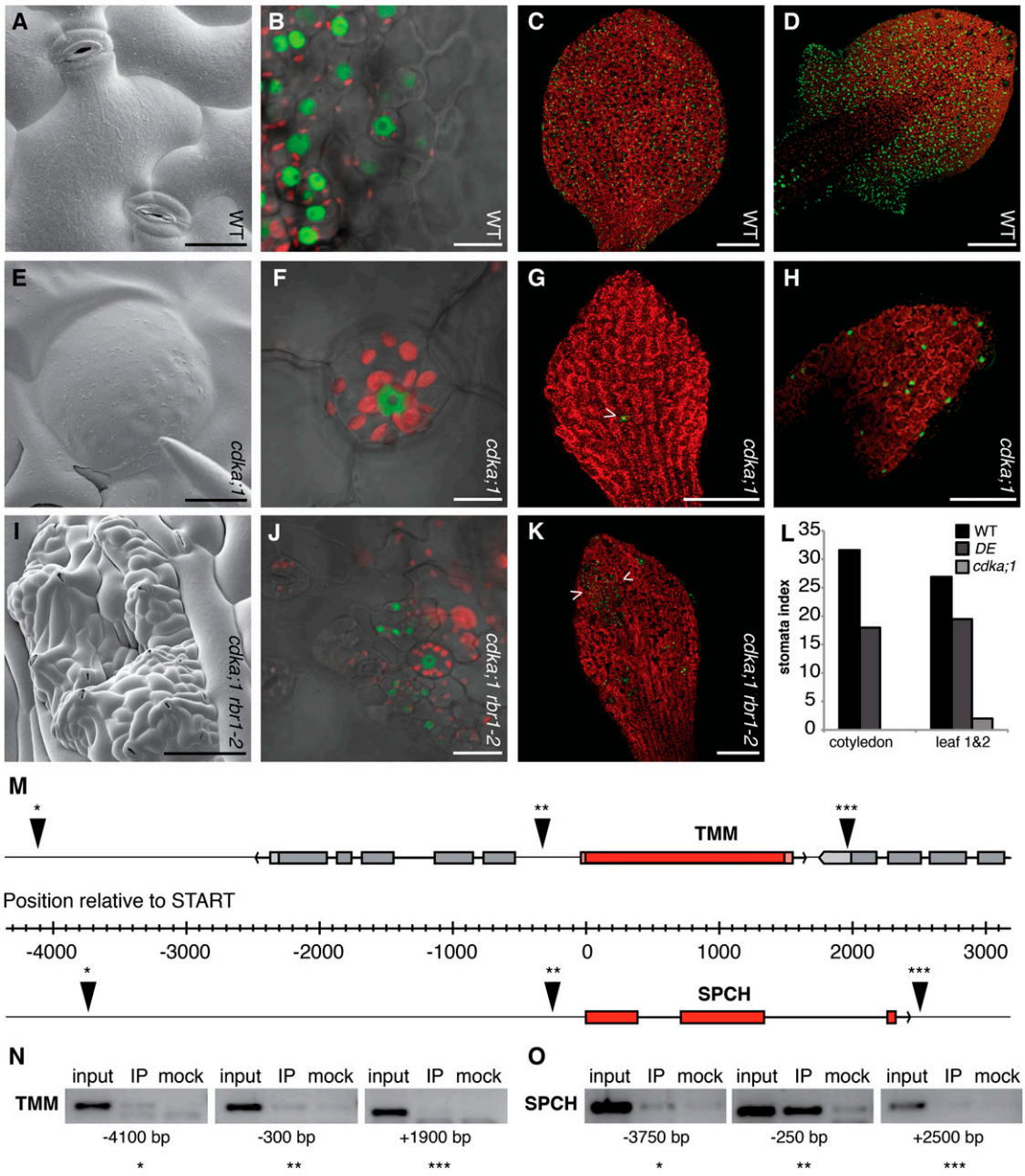

Figure 5. The Interplay between CDKA;1 and RBR1 Regulates Formative Divisions in the Stomata Lineage.

(A) Scanning electron micrographs of two stomata each comprised of two guard cells in the wild type (WT).
(B) Expression of the stomatal lineage marker Pro_{TMM}:*YFP* (green fluorescence) in the stomata lineage. Guard mother cells and guard cells contain chloroplasts as seen by red fluorescence.
(C) and **(D)** The stomata lineage marked by *TMM* expression in wild-type cotyledons **(C)** and in young wild-type rosette leaves **(D)**.
(E) and **(F)** Scanning electron micrographs of an arrested guard mother cell **(E)** in *cdka;1*$^{-/-}$ as indicated by *TMM* expression and the presence of chloroplasts **(F)**.
(G) and **(H)** The stomata lineage is not or rarely (arrowhead) activated in cotyledons of *cdka;1*$^{-/-}$ mutants as revealed by *TMM* expression (green) **(G)** and very rarely established in true leaves of *cdka;1*$^{-/-}$ mutants **(H)**.
(I) Scanning electron micrographs of *cdka;1 rbr1;2* double mutants, in which the activation of the stomatal lineage is partly restored in cotyledons.
(J) The *TMM* marker is strongly expressed in islands of overproliferating cells in *cdka;1 rbr1;2* double mutants.
(K) These islands can be surrounded by areas of *TMM*-negative cells and consist of stomata mixed with small meristematic cells.
(L) Stomata indices decrease from the wild type, to the weak loss-of-function *cdka;1* mutant *DE* and are very low in homozygous *cdka;1*$^{-/-}$ null mutants.

E2FA (Figure 4B). However, no enrichment beyond the level of the negative control could be obtained for the six above-tested SHR and SCR target genes using the E2FA antibody in ChIP experiments (Figure 4B). Thus, while genes with a direct role in cell cycle regulation are controlled by both RBR1 and E2F, the regulation of genes involved in cell differentiation was an E2F-independent function of RBR1. Thus, cell proliferation and cell differentiation are directly connected by RBR1.

The Interplay between CDKA;1 and RBR1 Also Regulates Formative Divisions in Aerial Structures

Finally, we wanted to know whether the role of RBR1 in the asymmetric cell division is specific to the cortex-endodermis initial daughter divisions or represents a general principle of formative cell divisions in *Arabidopsis*. Therefore, we analyzed stomata development in hypomorphic and *cdka;1* null mutants. Indeed, the number of stomata per mm^2 was significantly reduced in *cdka;1* mutants (see Supplemental Table 2 online). In addition, *DE* hypomorphic *cdka;1* mutant plants showed 4% undivided guard mother cells of all stomata as identified by their round shape, the presence of chloroplast, and the expression of stomatal lineage marker *TOO MANY MOUTHS* (*TMM*) that marks meristemoids and their progeny (Nadeau and Sack, 2002) (Figures 5A to 5D; see Supplemental Table 2 online). The occurrence of undivided guard mother cells increased to 80% of all stomata and guard mother cells in homozygous *cdka;1* null mutants, demonstrating that CDKA;1 is involved in the last symmetric cell division during stomatal development (Figures 5E to 5H; see Supplemental Table 2 online). This function was confirmed by the observation that expression of *CDKA;1* from the *TMM* promoter could partially rescue the previously reported arrest of guard mother cell division in *cdkb1;1 cdkb1;2* double mutants (see Supplemental Figures 4A to 4C online) (Xie et al., 2010).

To address whether asymmetric divisions that occur early during stomatal development are also affected by a reduction of CDKA;1 activity, we determined the stomatal indices in *DE* hypomorphic *cdka;1* mutants and *cdka;1* null mutants. The stomatal index is the percentage of stomata per all epidermal cells (including stomata). If symmetric and asymmetric divisions were equally affected in the mutants, the stomatal index should stay the same as that of the wild type or is even expected to slightly increase, since the stomatal lineage contributes to ~70% of all epidermal cells (Geisler et al., 2000). However, the stomatal index of the *DE* hypomorphic mutant was 18 for cotyledons and 19 for the first two rosette leaves and, hence, significantly lower ($P < 0.001$) than that of wild-type plants with a stomatal index of 32 for cotyledons and 27 for the first two rosette leaves (Figure 5L). This effect became even more striking in homozygous *cdka;1* mutants: In contrast with the wild type, the stomatal lineage was not activated in cotyledons (Figures 5G and 5L). On true leaves, few *TMM*-positive cells could be identified and stomata were only rarely formed (Figures 5H and 5L). Similar to the root, the defects during stomatal development could be reduced by expression of *CDKB1;1* under the *CDKA;1* promoter (see Supplemental Table 2 online). Importantly, the mutant phenotype was rescued when RBR1 was depleted (Figures 5I to 5K; see Supplemental Table 2 online). Thus, the interplay between CDKA;1 and RBR1 also regulates formative cell divisions during stomatal development.

Next, we asked whether RBR1 would also bind to genes involved in stomata differentiation. A key candidate would be the transcription factor SPEECHLESS (SPCH), which acts early in setting up a stomata lineage and is necessary and sufficient for the formation of stomata (MacAlister et al., 2007). While promoter fragments for the receptor kinase TMM could not be amplified by ChIP-PCR, one fragment of the SPCH promoter that was close to the transcriptional start site could readily be amplified after precipitation of RBR1-bound chromatin (Figures 5M and 5N). Thus, similar to the root, formative divisions in aerial structures are regulated by the interplay between CDKA;1 and RBR1, with RBR1 binding to differentiation genes.

DISCUSSION

Here, we have shown that formative divisions in the root and shoot depend on the level of CDKA;1 activity. This gives rise to a threshold model for formative cell divisions (Figure 6A). At low CDK levels, for instance, in the triple *cdk* mutant *cdka;1 cdkb1;1 cdkb1;2*, cell cycle progression is completely blocked (Nowack et al., 2012). At medium levels (e.g., in hypomorphic *cdka;1* mutants), RBR1 can be sufficiently inhibited to allow symmetric cell divisions. However, this reduced CDK activity is not enough to fully liberate cell differentiation genes from the repression of RBR1; hence, asymmetric divisions are specifically compromised. At high levels of CDK activity (i.e., in plants with functional CDKA;1 and CDKB1s), RBR1 can be completely inactivated, allowing the rapid execution of asymmetric divisions.

In turn, this mechanism allows asymmetric divisions to be developmentally programmed by providing positional cues for high kinase activity levels (Figure 6B). In the root meristem, this might be seen in the specific expression of *CYCD6;1* in the

Figure 5. (continued).

(M) The genomic region of *TMM* (top) and *SPCH* (below), both in red with neighboring genes in gray, exons depicted as filled rectangles and introns as lines. The orientation of the genes is given in the 5′ to 3′ direction and indicated with an arrowhead. The origin of the ruler indicates the translational start. ChIP fragments are shown by a triangle with one, two, or three asterisks corresponding to the PCR fragments shown in **(N)** and **(O)**.

(N) RBR1 does not bind to the promoter of the receptor kinase, as judged by ChIP of three different elements in the *TMM* genomic region. Amplified fragments corresponding to the genomic region shown in **(M)** are indicated with one, two, or three asterisks.

(O) RBR1 specifically binds to a promoter element shortly before the translational start of *SPCH*. Amplified fragments corresponding to the genomic region shown in **(M)** are indicated with one, two, or three asterisks.

Bars = 20 μm in **(A)**, **(E)**, and **(J)**, 10 μm in **(B)** and **(F)**, 100 μm in **(D)**, **(H)**, and **(I)**, and 250 μm in **(C)**, **(G)**, and **(K)**. IP = immuno precipitation in **(N)** and **(O)**.

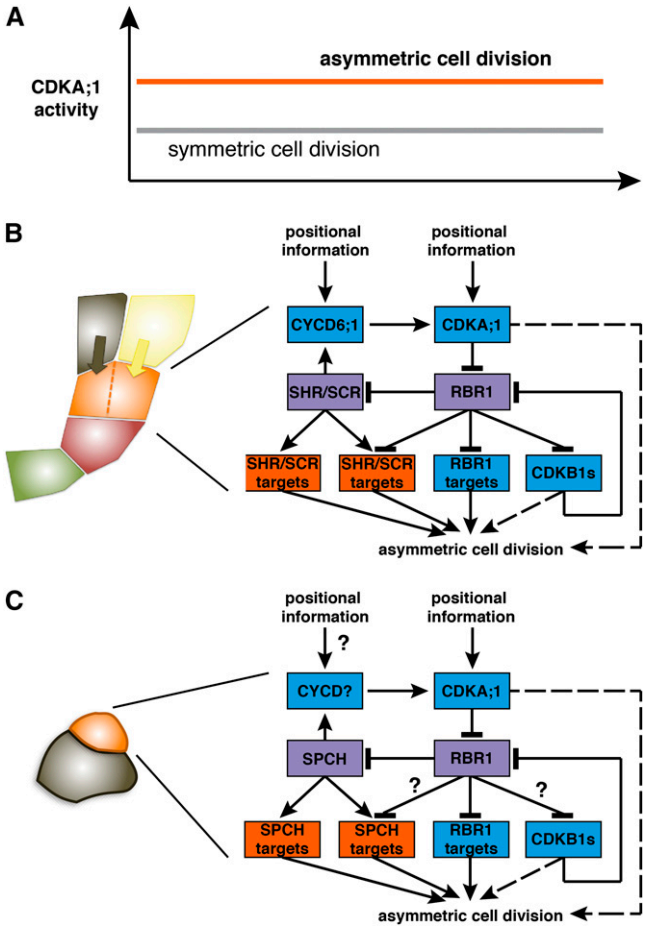

Figure 6.

(A) Model of asymmetric cell division in *Arabidopsis*. Of central importance is RBR1, which inhibits both cell cycle genes, such as *MCM5*, and cell differentiation genes, such as *SCL3*. At low levels of CDKA;1 activity (i.e., low levels of RBR1 inactivation), symmetrical cell divisions can occur, but inhibition of cell differentiation genes is only released at high levels of CDKA;1 activity (i.e., high levels of RBR1 inactivation), leading to asymmetric divisions.

(B) High levels of CDK activity in the initial daughter (orange) are directed by developmental cues (e.g., by the position-dependent activation of *CYCD6;1* that is also regulated by SCR and SHR). In addition, other positional cues appear to guide CDKA;1 activity to promote the division of the upper-most initial daughter and thus likely involve cues from the already specified endodermis (black) and cortex (yellow) layers. Green shading, quiescent center cell; red, initial. Model of molecular circuitry during asymmetric divisions in the cortex-endodermis initial daughter cell. RBR1 and SHR/SCR (violet boxes) integrate cell differentiation (genes with orange boxes) with cell cycle control (genes in blue boxes). The activation of genes required for asymmetric cell divisions involves double negative-feedback loops, resulting in a feed-forward mechanism that is likely to generate hysteresis. SHR/SCR activate CYCD6;1, which then inactivates their repressor (RBR1). Whether CDKs (i.e., CDKA;1 and CDKB1) also participate directly in the regulation of the symmetric division, for instance, by regulating the spindle orientation, is not clear and is indicated by a hatched line.

(C) Model of formative division during the stomata lineage. The formative division restores the meristemoid cell (orange) and generates a neighboring epidermal cell (black). High levels of CDKA;1 activity in the meristemoid mother cell and/or meristemoid (orange) are required to initiate formative divisions in the stomata lineage. Similar to the root, the major substrate appears to be RBR1. Whereas CDKB1s have a role during the symmetric division of a guard mother cell, it is not clear whether they also participate during formative divisions (question mark). The basic helix-loop-helix transcription factor SPCH is regulated by RBR1. In analogy to the function of SHR and SCR, it seems likely that SPCH directly regulates the expression of cell cycle genes, such as D-type cyclins. However, there is currently no molecular evidence for this (question mark). It is also not clear whether SPCH targets are regulated by RBR1 (question mark). Similar to the root, it is remains to be seen whether CDKs regulate other aspects of asymmetric divisions (e.g., the polar localization of cell fate determinants) (hatched line).

cortex-endodermis initial daughter cell (Sozzani et al., 2010) and in the fact that the formative division of the cortex-endodermis initial daughter cell is rapid. *CYCD6;1* is regulated by the SHR/SCR pathway (Sozzani et al., 2010), but notably, we identified SCR itself as an RBR1 target. Thus, SHR/SCR acts in a double negative feedback loop, since CYCD6;1 activates CDKA;1, which in turn phosphorylates and inhibits RBR1, which itself acts as a transcriptional repressor of SCR (Figure 6B).

This wiring resembles the recently identified wiring of RBR1 in a pathway that regulates entry into S phase in which RBR1 directly represses the expression of the F-box protein FBL17 that mediates the degradation of CDK inhibitors (Zhao et al., 2012). A central feature of this S phase regulatory cascade is hysteresis that arises through the connection of at least two negative feedback loops (Ferrell, 2002). Thus, it is conceivable that the here-identified wiring during formative division will generate hysteresis. Hysteresis is important to reach stable decisions in biology, since the activity levels to initiate a process (e.g., DNA replication) are higher than the levels to continue this process. In the case of the cell cycle, hysteresis contributes to its unidirectionality (i.e., the replication of nuclear DNA only once per cell cycle and an ordered progression of mitosis in which chromosomes typically do not fluctuate between condensation and decondensation) (Tyson and Novak, 2008).

In addition, a second double negative feedback loop centered on B1-type CDKs appears to operate during S-phase entry and the execution of formative divisions. CDKB1s were found to have some activity against RBR1 and can partially compensate for the loss of CDKA;1 (Nowack et al., 2012). The *cdkb1;1 cdkb1;2* double mutant also showed a delayed division of the cortex-endodermis initial daughter cell, underlining their contribution for the formative division. Remarkably, *CDKB1;1* and *CDKB1;2* are also under the control of RBR1 (Nowack et al., 2012), hence contributing, although to a lesser extent than CDKA;1, to the hysteretical behavior of the system.

The importance of RBR1 for stomata formation has already previously been demonstrated (Borghi et al., 2010). Our finding that SPCH is also bound by RBR1 suggests that a similar regulatory cascade controls formative divisions during stomata lineage, although it remains to be seen whether SPCH directly regulates the expression of cell cycle regulators. By analogy, key candidates here are D-type cyclins, such as *CYCD4;1* and

CYCD4;2, that have already been implicated in the regulation of the divisions that initiate the stomata lineage (Figure 6C) (Kono et al., 2007).

A central question is how the regulatory cascade is initiated that then results in a formative division of the cortex-endodermis initial cell. One cue comes from the observation that *CYCD6;1* becomes expressed in the additional cells between initial and endodermis/cortex in hypomorphic *cdka;1* mutants. Consistently, we see that the promoter of *CYCD6;1* is not, or at least not strongly, bound by RBR1. Again, this resembles known patterns of cell cycle regulation. In mammals, entry into S phase is initiated by phosphorylation of Rb by the two kinases Cdk4 and Cdk6 that pair with D-type cyclins (Weinberg, 1995; Dyson, 1998; Sherr and Roberts, 1999). Partially phosphorylated Rb cannot sufficiently repress CycE, and CycE in conjunction with Cdk2 will then fully phosphorylate Rb, causing the derepression of many genes required for DNA replication, such as *PCNA*. Thus, it seems likely that such a two-step process also operates in root meristems, but it remains to be seen which other cyclin or cell cycle regulator is in charge of RBR1 inactivation.

In addition to the expression of *CYCD6;1* in the daughter cell, positional information appears to direct the formative division, since only the uppermost cell, which was in direct contact with the already specified endodermis and cortex layers, eventually divided asymmetrically, although *CYCD6;1* was expressed in all additional daughter cells in hypomorphic *cdka;1* mutants. Thus, it is tempting to speculate that the system is further biased by a cue that comes from the endodermis and/or cortex layer. Evidence for local signaling in the root in which a direct cell-to-cell contact provides fate information comes from ablation experiments (van den Berg et al., 1997). Such a cue could lead to the expression/activation of another cell cycle regulator, especially since *cycd6;1* mutants only showed a slight retardation in the execution of a formative divisions. Although a delay of the formative division did not interfere with later differentiation steps as seen in *cycd6;1* mutants or, more pronouncedly, in hypomorphic *cdka;1* alleles, a fast execution of the formative division assures that meristem integrity is maintained (i.e., that the different populations of proliferating cells within the meristem coordinate their cell division rates and that cell differentiation proceeds with the same pace as cell production).

Interestingly, asymmetric cell divisions in *Drosophila melanogaster* have been previously found to depend on the dose of Cdk1 that is homologous to CDKA;1 (Tio et al., 2001). However, the underlying mechanisms of Cdk action in *Drosophila* versus *Arabidopsis* appear to be different. Cdk1 in *Drosophila* is required for the asymmetric localization of an apical-cortical complex at interphase, which then directs the apical-basal orientation of the mitotic spindle as well as the basal/cortical localization of cell fate determinants during mitosis. By contrast, we found here that CDKA;1 operates through a transcriptional regulatory system. However, we currently cannot exclude that CDK activity is also required for proper spindle orientation in the cortex-endodermis initial daughter cell, and it remains to be seen how the generation of a local peak in kinase activity through the double-negative feedback loops identified in this study is further used in the regulation of asymmetric cell divisions (e.g., by affecting cell polarity and/or the cytoskeleton).

METHODS

Plant Material and Growth Conditions

The *Arabidopsis thaliana* plants used in this study were either grown on soil (16 h light) or in vitro on half-strength Murashige and Skoog medium (MS; Sigma Aldrich) containing 0.5% Suc (16 h light) in a growth chamber. The accession Columbia-0 was used as the wild type. *cdka;1* and *rbr1*-2 mutant alleles were described previously (Ebel et al., 2004; Nowack et al., 2006). The hypomorphic *cdka;1* mutants (*D* and *DE*) have been characterized (Dissmeyer et al., 2007, 2009). T-DNA insertion lines for CDKB1;1 and CDKB1;2 have been described (Nowack et al., 2012). The T-DNA allele for CYCD6;1 was described previously (Sozzani et al., 2010). The Pro_{RBR1}:*RBR1-mRFP*–expressing plants have been described (Ingouff et al., 2006). The *TMM* promoter was described previously (Nadeau and Sack, 2002). The Pro_{SCR}:*SCR:YFP* (for yellow fluorescent protein) and PRO_{CO2}:*H2B:YFP* lines were presented previously (Heidstra et al., 2004). All genotypes were determined by PCR, and primers are indicated in Supplemental Table 3 online.

Microscopy

For whole-mount embryo preparation, siliques were dissected with needles, in such a manner that the ovules remained connected to the placenta. Dissected siliques were fixed on ice in FAA (10:7:2:1 ethanol:distilled water: acetic acid:formaldehyde; 37%) for 30 min. After that, the siliques were hydrated in a graded ethanol series to 50 nM $NaPO_4$, pH 7.2, and mounted on microscope slides in a clearing solution of 8:2:1 chloral hydrate:water: glycerol. Embryo phenotypes were analyzed with a Zeiss Imager.Z1 with AxioCam MRm. The software used was AxioVision Rel. 4.8.2.

For root cell wall staining, entire 5- to 12-d-old seedlings were stained with propidium iodide (Invitrogen; stock 1 mg/mL, 100× dilution) in water for 3 to 4 min and rinsed afterwards once in water. Confocal laser scanning microscopy was performed on an inverted Zeiss LSM 510 confocal microscope. Excitation and detection windows were set as follows: YFP, 488 nm, 500 to 600 nm; propidium iodide, 488 nm, 500 to 550 nm.

For visualization of the Casparian strips, roots of 10- to 12-d-old seedlings were used. Seedlings were incubated in 0.24 N HCl in 20% methanol at 57°C for 15 min. This solution was replaced with 7% NaOH in 60% ethanol for 15 min at room temperature. Roots were then rehydrated for 5 min each in 40, 20, and 10% ethanol and infiltrated for 15 min in 5% ethanol and 25% glycerol. Roots were mounted in 50% glycerol for microscopy analysis. To detect the apoplastic barrier, seedlings were incubated in the dark for 10 min in a fresh solution of 15 μM (10 μg/mL) propidium iodide and rinsed two times in water (Alassimone et al., 2010). Confocal laser scanning microscopy was performed on an inverted Leica SP2 and Zeiss LSM 700 confocal microscope. Excitation and detection windows were set as follows: green fluorescent protein, 488 nm, 500 to 600 nm; propidium iodide 488 nm, 500 to 550 nm.

Stomata numbers were determined on cotyledons or the two first true leaves of wild-type or mutant plants as indicated. Plants were grown well-spaced on agar plates with half-strength MS medium containing 0.5% Suc, pH 5.8. Cotyledons and true leaves were collected 21 d after germination, fixed in a 100% watery ethanol solution, and cleared and mounted in lactic acid. The samples were viewed using a Zeiss Axiophot microscope with Nomarski optics. Stomata density was determined by counting the stomata on two defined areas per leaf. The stomata index was calculated as described before by dividing the number of guard cells (number of stomata multiplied by two to correct for the presence of two guard cells) by the total number of cells (pavement cells + guard cells) (Rymen et al., 2010).

Histology

For GUS (for β-glucuronidase) assays, 5-d-old seedlings were directly collected in staining buffer with X-Gluc and infiltrated under vacuum for

5 to 10 min at room temperature. The samples were incubated at 37°C overnight. After one washing step in ethanol (70%) for 30 min, the seedlings were mounted in chloral hydrate for 3 h. Staining buffer was prepared as follows: 0.2% Triton, 50 mM $NaPO_4$, 2 mM Ferro-K, 2 mM Ferri-K, and 2 mM X-Gluc, filled up with water.

Expression Constructs

The Gateway Entry clone of CDKA;1-YFP (Nowack et al., 2007) was recombined into the destination vector pAM-PAT-GW-ProTMM (Weinl et al., 2005). The resulting binary plant expression vector, which confers phosphinotricine (BASTA; Bayer Cropscience) resistance, was retransformed into *Agrobacterium tumefaciens* GV3101-pMP90RK. Heterozygous plants for *cdka;1-1* and *rbr1-2* and homozygous plants for *cdkb1;1 cdkb1;2* were transformed.

Kinase Assay

To clone *CYCD6;1*, total RNA was extracted from flower buds using NucleoSpin RNA Plant (Macherey-Nagel). First-stranded cDNA was synthesized using SuperScript III reverse transcriptase (Invitrogen) with oligo (dT)-AP_M13 according to the manufacturer's instructions (all primer sequences are in Supplemental Table 3 online). *CYCD6;1* cDNA was amplified first with primers CYCD6;1_s1 and M13-forward, followed by primers CYCD6;1_s1 and CYCD6;1_as2. The resulting PCR products were cloned using a CloneJET PCR cloning kit (Fermentas) and sequenced. To express CYCD6;1 in *E.scherichia coli*, cDNA was amplified by sequential PCR first using attB1Ad-CYCD6;1_s and attB2Ad-CYCD6;1_as, followed by the attB1 adapter primer and attB2 adapter primer. The PCR product was cloned into the pDONR223 vector (Invitrogen). A recombination reaction was performed between the resulting entry clone and a destination vector pHMGWA (Busso et al., 2005). To express CDKA;1 hypomorphic alleles in *E. coli*, site-directed mutagenesis was performed using StrepIII-CDKA;1 in *pCDFDuet-Cak1* (Harashima and Schnittger, 2012) as a template of PCR. For D, the 5′ half was amplified with the ACYCDuetUP1 primer and the ND35; 3′ half was amplified with ND34 and the DuetDOWN1 primer. For DE, the ACYCDuetUP1 primer and ND04 and ND03 and the DuetDOWN1 primer were used. The 5′ and 3′ half of StrepIII-CDKA;1 were fused by PCR using the ACYCDuetUP1 and DuetDOWN1 primers. The resulting PCR products were digested by *Nco*I and *Not*I and cloned into the *Nco*I-*Not*I site of *pCDFDuet-Cak1*. CDK-cyclin complexes were expressed and purified from *E. coli* as described previously (Harashima and Schnittger, 2012). $p13^{suc1}$-associated kinases were purified as described previously (Harashima and Sekine, 2011) from 14-d-old Col-0, *D*, and *DE* seedlings grown on half-strength MS plates containing 0.5% Suc. CDK-cyclin complexes were processed for kinase assays as described previously (Harashima and Sekine, 2011) using Histone H1 as a substrate.

ChIP

ChIP was performed as previously described (Berr et al., 2010; Bouyer et al., 2011; Zhao et al., 2012). Two-week-old seedlings of Pro_{RBR1}:*RBR1*:*mRFP* growing on 0.5 MS plates were used. Chromatin was sheared with a Bioruptor sonicator (Cosmo Bio) twice for 15 min with a 50% duty cycle and high power output to obtain 200- to 1000-bp DNA fragments. Immunoprecipitation was performed using the DsRed polyclonal antibody (Clontech) together with Protein A-magnetic beads (Millipore). The E2FA antibody was described previously (Heyman et al., 2011). Negative controls were performed without antibody. DNA was recovered using Magna ChIP spin filters according to the manufacturer's instructions (Millipore). Then, 0.5 or 1 μL of a one-fifth dilution of ChIP DNA was analyzed by ChIP PCR or quantitative real-time PCR using gene-specific primers, respectively (see Supplemental Table 3 online). Two biological and three technical replicates were performed for ChIP–quantitative PCR using PCNA1 and MCM5 as positive controls and heterochromatic region primers as a negative control (see Supplemental Table 3 online).

Statistical Analyses

A multinomial distribution was generated by taking the sum of the count data, followed by fitting a generalized linear model, incorporating a log-linear link function to test for the difference of the supernumerary cortex-endodermis initial daughter cells in hypomorphic mutants versus wild-type plants. For the comparison of different time points (Figure 3), multinomial distributions were determined for each of the multinominate values. For statistical analyses of stomata indices (Figure 3), a binomial distribution was generated by taking the sum of the count data, followed by fitting a generalized linear model, incorporating a logit link function.

Accession Numbers

Sequence data from this article can be found in the Arabidopsis Genome Initiative or GenBank/EMBL databases under the following accession numbers: CDKA;1 has the Arabidopsis Genome Initiative code At3g48750. The T-DNA insertion line for the *cdka;1* mutant allele used (cdka;1-1) is Salk_106809.34.90.X. For RBR1 (At3g12280), the T-DNA insertion line used was SALK_002946. CDKB1;1 (At3g54180) mutants from the SALK_073457 line and CDKB1;2 (At2g38620) mutants from the SALK_133560 line were used. For the ChIP experiments, the following genes with their respective Arabidopsis Genome Initiative code were used: CYCD6;1 (At4g03270), MCM5 (At2g07690), MGP (At1g03840), NUC (At5g44160), PCNA1 (At1g07370), SCL3 (At1g50420), SCR (At3g54220), SPCH (At5g53210), and TMM (At1g80080).

Supplemental Data

The following materials are available in the online version of this article.

Supplemental Figure 1. Casparian Strip Formation Is Not Affected in Weak *cdka;1* Alleles.

Supplemental Figure 2. Cortex and Endodermis Differentiation.

Supplemental Figure 3. RBR1 ChIP.

Supplemental Figure 4. CDKA;1 Overexpression Partially Rescues *cdkb1;1 cdkb1;2* Stomata Defects.

Supplemental Table 1. Time Frame of Cortex-Endodermis Initial Daughter Division.

Supplemental Table 2. Stomata Density in *cdka;1* Mutants.

Supplemental Table 3. Oligonucleotides.

ACKNOWLEDGMENTS

We thank Tom Beeckman and Pierre Hilson (VIB) for the $Pro_{CYCD6;1}$:*GUS* reporter line, Frédéric Berger (National University of Singapore) for the Pro_{RBR1}:*RBR1-mRFP*–expressing plants, Renze Heidstra (University of Wageningen) for the *SCR* and *CO2* marker lines, Fred Sack (University of British Columbia) for the *TMM* promoter construct, and Lieven De Veylder, Vlaams Instituut voor Biotechnologie, for the E2FA antibody. We thank Marnik Vuylsteke, Vlaams Instituut voor Biotechnologie, for help with the statistical analysis and Jonathan Bramsiepe for assistance in producing *cdka;1* $Pro_{CDKA;1}$:$CDKA;1^{T14D;Y15E}$ *rbr1* plants. We also thank Annick Bleys for critical reading and helpful comments on the article. This work was supported by an EMBO Long-Term Fellowship (to M.K.N.), by Grant "Action Thématique et Incitative sur Programme" from the Centre

National de la Recherche Scientifique (to A.S.), by a European Union Interreg IV project (to A.S.), and by a European Research Council Starting Independent Researcher grant (to A.S.).

AUTHOR CONTRIBUTIONS

A.K.W., M.K.N., D.B., X.A.Z., H.H., N.D., N.G., and A.S. conceived and designed the experiments. A.K.W., M.K.N., D.B., X.A.Z., H.H., S.N., F.D.W., and N.D. performed the experiments. A.K.W., M.K.N., D.B., X.A.Z., H.H., S.N., F.D.W., N.D., N.G., and A.S. analyzed the data. A.K.W., M.K.N., N.G., and A.S. wrote the article.

Received August 28, 2012; revised September 22, 2012; accepted October 2, 2012; published October 26, 2012.

REFERENCES

Abrash, E.B., and Bergmann, D.C. (2009). Asymmetric cell divisions: A view from plant development. Dev. Cell **16:** 783–796.

Alassimone, J., Naseer, S., and Geldner, N. (2010). A developmental framework for endodermal differentiation and polarity. Proc. Natl. Acad. Sci. USA **107:** 5214–5219.

Andersen, S.U., Buechel, S., Zhao, Z., Ljung, K., Novák, O., Busch, W., Schuster, C., and Lohmann, J.U. (2008). Requirement of B2-type cyclin-dependent kinases for meristem integrity in *Arabidopsis thaliana*. Plant Cell **20:** 88–100.

Benfey, P.N., and Scheres, B. (2000). Root development. Curr. Biol. **10:** R813–R815.

Bergmann, D.C., and Sack, F.D. (2007). Stomatal development. Annu. Rev. Plant Biol. **58:** 163–181.

Berr, A., McCallum, E.J., Ménard, R., Meyer, D., Fuchs, J., Dong, A., and Shen, W.H. (2010). *Arabidopsis* SET DOMAIN GROUP2 is required for H3K4 trimethylation and is crucial for both sporophyte and gametophyte development. Plant Cell **22:** 3232–3248.

Borghi, L., Gutzat, R., Fütterer, J., Laizet, Y., Hennig, L., and Gruissem, W. (2010). *Arabidopsis* RETINOBLASTOMA-RELATED is required for stem cell maintenance, cell differentiation, and lateral organ production. Plant Cell **22:** 1792–1811.

Boudolf, V., Barrôco, R., Engler, Jde.A., Verkest, A., Beeckman, T., Naudts, M., Inzé, D., and De Veylder, L. (2004). B1-type cyclin-dependent kinases are essential for the formation of stomatal complexes in *Arabidopsis thaliana*. Plant Cell **16:** 945–955.

Bouyer, D., Roudier, F., Heese, M., Andersen, E.D., Gey, D., Nowack, M.K., Goodrich, J., Renou, J.P., Grini, P.E., Colot, V., and Schnittger, A. (2011). Polycomb repressive complex 2 controls the embryo-to-seedling phase transition. PLoS Genet. **7:** e1002014.

Busso, D., Delagoutte-Busso, B., and Moras, D. (2005). Construction of a set Gateway-based destination vectors for high-throughput cloning and expression screening in *Escherichia coli*. Anal. Biochem. **343:** 313–321.

De Smet, I., and Beeckman, T. (2011). Asymmetric cell division in land plants and algae: The driving force for differentiation. Nat. Rev. Mol. Cell Biol. **12:** 177–188.

Dissmeyer, N., Nowack, M.K., Pusch, S., Stals, H., Inzé, D., Grini, P.E., and Schnittger, A. (2007). T-loop phosphorylation of *Arabidopsis* CDKA;1 is required for its function and can be partially substituted by an aspartate residue. Plant Cell **19:** 972–985.

Dissmeyer, N., Weimer, A.K., Pusch, S., De Schutter, K., Alvim Kamei, C.L., Nowack, M.K., Novak, B., Duan, G.L., Zhu, Y.G., De Veylder, L., and Schnittger, A. (2009). Control of cell proliferation, organ growth, and DNA damage response operate independently of dephosphorylation of the *Arabidopsis* Cdk1 homolog CDKA;1. Plant Cell **21:** 3641–3654.

Dyson, N. (1998). The regulation of E2F by pRB-family proteins. Genes Dev. **12:** 2245–2262.

Ebel, C., Mariconti, L., and Gruissem, W. (2004). Plant retinoblastoma homologues control nuclear proliferation in the female gametophyte. Nature **429:** 776–780.

Ferrell, J.E. Jr. (2002). Self-perpetuating states in signal transduction: positive feedback, double-negative feedback and bistability. Curr. Opin. Cell Biol. **14:** 140–148.

Geisler, M.D., Nadeau, J.A., and Sack, F.D. (2000). Oriented asymmetric divisions that generate the stomatal spacing pattern in arabidopsis are disrupted by the too many mouths mutation. Plant Cell **12:** 2075–2086.

Gutzat, R., Borghi, L., and Gruissem, W. (2012). Emerging roles of RETINOBLASTOMA-RELATED proteins in evolution and plant development. Trends Plant Sci. **17:** 139–148.

Harashima, H., and Schnittger, A. (2010). The integration of cell division, growth and differentiation. Curr. Opin. Plant Biol. **13:** 66–74.

Harashima, H., and Schnittger, A. (2012). Robust reconstitution of active cell-cycle control complexes from co-expressed proteins in bacteria. Plant Methods **8:** 23.

Harashima, H., and Sekine, M. (2011). Measurement of plant cyclin-dependent kinase activity using immunoprecipitation-coupled and affinity purification-based kinase assays and the baculovirus expression system. Methods Mol. Biol. **779:** 65–78.

Heidstra, R., Welch, D., and Scheres, B. (2004). Mosaic analyses using marked activation and deletion clones dissect Arabidopsis SCARECROW action in asymmetric cell division. Genes Dev. **18:** 1964–1969.

Heyman, J., Van den Daele, H., De Wit, K., Boudolf, V., Berckmans, B., Verkest, A., Alvim Kamei, C.L., De Jaeger, G., Koncz, C., and De Veylder, L. (2011). *Arabidopsis* ULTRAVIOLET-B-INSENSITIVE4 maintains cell division activity by temporal inhibition of the anaphase-promoting complex/cyclosome. Plant Cell **23:** 4394–4410.

Ingouff, M., Jullien, P.E., and Berger, F. (2006). The female gametophyte and the endosperm control cell proliferation and differentiation of the seed coat in *Arabidopsis*. Plant Cell **18:** 3491–3501.

Knoblich, J.A. (2010). Asymmetric cell division: Recent developments and their implications for tumour biology. Nat. Rev. Mol. Cell Biol. **11:** 849–860.

Kono, A., Umeda-Hara, C., Adachi, S., Nagata, N., Konomi, M., Nakagawa, T., Uchimiya, H., and Umeda, M. (2007). The *Arabidopsis* D-type cyclin CYCD4 controls cell division in the stomatal lineage of the hypocotyl epidermis. Plant Cell **19:** 1265–1277.

MacAlister, C.A., Ohashi-Ito, K., and Bergmann, D.C. (2007). Transcription factor control of asymmetric cell divisions that establish the stomatal lineage. Nature **445:** 537–540.

Menges, M., de Jager, S.M., Gruissem, W., and Murray, J.A. (2005). Global analysis of the core cell cycle regulators of *Arabidopsis* identifies novel genes, reveals multiple and highly specific profiles of expression and provides a coherent model for plant cell cycle control. Plant J. **41:** 546–566.

Morgan, D.O. (1997). Cyclin-dependent kinases: Engines, clocks, and microprocessors. Annu. Rev. Cell Dev. Biol. **13:** 261–291.

Nadeau, J.A., and Sack, F.D. (2002). Control of stomatal distribution on the *Arabidopsis* leaf surface. Science **296:** 1697–1700.

Nowack, M.K., Grini, P.E., Jakoby, M.J., Lafos, M., Koncz, C., and Schnittger, A. (2006). A positive signal from the fertilization of the egg cell sets off endosperm proliferation in angiosperm embryogenesis. Nat. Genet. **38:** 63–67.

Nowack, M.K., Harashima, H., Dissmeyer, N., Zhao, X., Bouyer, D., Weimer, A.K., De Winter, F., Yang, F., and Schnittger, A. (2012).

Genetic framework of cyclin-dependent kinase function in Arabidopsis. Dev. Cell **22:** 1030–1040.

Nowack, M.K., Shirzadi, R., Dissmeyer, N., Dolf, A., Endl, E., Grini, P.E., and Schnittger, A. (2007). Bypassing genomic imprinting allows seed development. Nature **447:** 312–315.

Pines, J. (1995). Cyclins and cyclin-dependent kinases: A biochemical view. Biochem. J. **308:** 697–711.

Pusch, S., Harashima, H., and Schnittger, A. (2012). Identification of kinase substrates by bimolecular complementation assays. Plant J. **70:** 348–356.

Rymen, B., Coppens, F., Dhondt, S., Fiorani, F., and Beemster, G.T. (2010). Kinematic analysis of cell division and expansion. Methods Mol. Biol. **655:** 203–227.

Sherr, C.J., and Roberts, J.M. (1999). CDK inhibitors: Positive and negative regulators of G1-phase progression. Genes Dev. **13:** 1501–1512.

Sozzani, R., Cui, H., Moreno-Risueno, M.A., Busch, W., Van Norman, J.M., Vernoux, T., Brady, S.M., Dewitte, W., Murray, J.A., and Benfey, P.N. (2010). Spatiotemporal regulation of cell-cycle genes by SHORTROOT links patterning and growth. Nature **466:** 128–132.

Ten Hove, C.A., and Heidstra, R. (2008). Who begets whom? Plant cell fate determination by asymmetric cell division. Curr. Opin. Plant Biol. **11:** 34–41.

Tio, M., Udolph, G., Yang, X., and Chia, W. (2001). cdc2 links the Drosophila cell cycle and asymmetric division machineries. Nature **409:** 1063–1067.

Tyson, J.J., and Novak, B. (2008). Temporal organization of the cell cycle. Curr. Biol. **18:** R759–R768.

Ubeda-Tomás, S., Federici, F., Casimiro, I., Beemster, G.T., Bhalerao, R., Swarup, R., Doerner, P., Haseloff, J., and Bennett, M.J. (2009). Gibberellin signaling in the endodermis controls Arabidopsis root meristem size. Curr. Biol. **19:** 1194–1199.

van den Berg, C., Willemsen, V., Hendriks, G., Weisbeek, P., and Scheres, B. (1997). Short-range control of cell differentiation in the *Arabidopsis* root meristem. Nature **390:** 287–289.

Van Leene, J., Boruc, J., De Jaeger, G., Russinova, E., and De Veylder, L. (2011). A kaleidoscopic view of the *Arabidopsis* core cell cycle interactome. Trends Plant Sci. **16:** 141–150.

Weinberg, R.A. (1995). The retinoblastoma protein and cell cycle control. Cell **81:** 323–330.

Weinl, C., Marquardt, S., Kuijt, S.J., Nowack, M.K., Jakoby, M.J., Hülskamp, M., and Schnittger, A. (2005). Novel functions of plant cyclin-dependent kinase inhibitors, ICK1/KRP1, can act non-cell-autonomously and inhibit entry into mitosis. Plant Cell **17:** 1704–1722.

Xie, Z., Lee, E., Lucas, J.R., Morohashi, K., Li, D., Murray, J.A., Sack, F.D., and Grotewold, E. (2010). Regulation of cell proliferation in the stomatal lineage by the *Arabidopsis* MYB FOUR LIPS via direct targeting of core cell cycle genes. Plant Cell **22:** 2306–2321.

Zhao, X., Harashima, H., Dissmeyer, N., Pusch, S., Weimer, A.K., Bramsiepe, J., Bouyer, D., Rademacher, S., Nowack, M.K., Novak, B., Sprunck, S., and Schnittger, A. (2012). A general G1/S-phase cell-cycle control module in the flowering plant *Arabidopsis thaliana*. PLoS Genet. **8:** e1002847.